R. Brighenti et alii, Frattura ed Integrità Strutturale, 20 (2012) 6-16; DOI: 10.3221/IGF-ESIS.20.01

Crack path dependence on inhomogeneities of material microstructure

Roberto Brighenti, Andrea Carpinteri, Andrea Spagnoli, Daniela Scorza
Department of Civil and Environmental Engineering & Architecture, University of Parma,
Viale Usberti, 181/A, 43124 Parma, Italy
spagnoli@unipr.it

ABSTRACT. Crack trajectories under different loading conditions and material microstructural features play an important role when the conditions of crack initiation and crack growth under fatigue loading have to be evaluated. Unavoidable inhomogeneities in the material microstructure tend to affect the crack propagation pattern, especially in the short crack regime. Several crack extension criteria have been proposed in the past decades to describe crack paths under mixed mode loading conditions. In the present paper, both the Sih criterion (maximum principal stress criterion) and the R-criterion (minimum extension of the core plastic zone) are adopted in order to predict the crack path at the microscopic scale level by taking into account microstress fluctuations due to material inhomogeneities. Even in the simple case of an elastic behaviour under uniaxial remote stress, microstress field is multiaxial and highly non-uniform. It is herein shown a strong dependence of the crack path on the material microstructure in the short crack regime, while the microstructure of the material does not influence the crack trajectory for relatively long cracks.

SOMMARIO. L'andamento dei percorsi di frattura sotto diverse condizioni di carico e caratteristiche microstrutturali del materiale ha un ruolo importante nella determinazione delle condizioni di nucleazione e propagazione a fatica della fessura. Inevitabili disomogeneità nella microstruttura del materiale tendono a influenzare il percorso di propagazione della fessura, particolarmente nel caso di fessure corte. In letteratura sono stati proposti numerosi criteri volti a descrivere i percorsi di frattura in condizioni di modo misto. Nel presente lavoro, sia il criterio di Sih (della massima tensione principale) che il criterio R (della minima estensione della zona plastica) sono stati adottati per predire i percorsi di frattura alla scala microscopica tenendo conto di fluttuazioni delle microtensioni dovute alle disomogeneità del materiale. Anche nel semplice caso di comportamento elastico del materiale in presenza di tensione monoassiale remota, il campo tensionale alla microscala risulta essere multiassiale e non uniforme. Viene evidenziata una significativa dipendenza del percorso di frattura nel caso di fessure corte dalla microstruttura del materiale, mentre nel caso di fessure lunghe tale dipendenza risulta trascurabile.

KEYWORDS. Crack path; Kinked crack; Microstress fluctuation; Material microstructure.

INTRODUCTION

The evaluation of fatigue crack growth at small scale is still an open problem. As a matter of fact, when the crack size is comparable with a characteristic length of the material (e.g. grain size in metallic materials), mechanical barriers to crack growth are produced by the material microstructure, and the plastic zone size at crack tip

happens to be comparable with the crack size, leading to the violation of the small-scale yielding hypothesis. The effects of the material microstructure on the crack growth at small scale [1] can be modelled by taking into account the non-uniform stress field induced by embedded inohomogeneities. Even for a uniform remote stress applied to the structural component, an oscillating stress field might develop at the microscale.
In the present paper, by using both the solution of a homogeneous elastic infinite plane with a circular elastic inclusion and the superposition principle, the stress field for a regular arrangement of inclusions is determined, and the corresponding mixed mode Stress Intensity Factors (SIFs) are computed. Crack paths are evaluated by applying both the maximum principal stress criterion (the Sih criterion [2, 3]) and the minimum plastic zone extension criterion (the R-criterion [4, 5]). The trajectory described by the crack tip is computed through an incremental method, where the Mode I and Mode II SIFs of the kinked crack are approximately evaluated as a function of the SIFs related to a projected straight crack. Finally, some examples related to metallic alloys are examined. It is shown that small-scale fluctuations of the stress field heavily affect the crack path for short cracks while, after reaching a transition point during the crack propagation process, such an influence disappears for sufficiently long cracks.

MICROSTRESS FIELD INDUCED BY MATERIAL INHOMOGENEITIES

Structural materials always present heterogeneity features due to either the composite nature of the materials (e.g. composite materials characterised by a matrix and a reinforcing phase; concrete-like materials having a cement-based paste with dispersion of aggregates of different sizes) or unavoidable inhomogeneities (e.g. metallic alloys composed by a base material and secondary inclusions), see Fig. 1. Due to such inhomogeneity characteristics, the stress field in the material at microscopic level might be non-uniform and multiaxial even if a uniaxial uniform remote stress is applied. A local fluctuation of the microstress field can play a crucial role in the crack path assessment for cracks having length comparable with a characteristic material length.

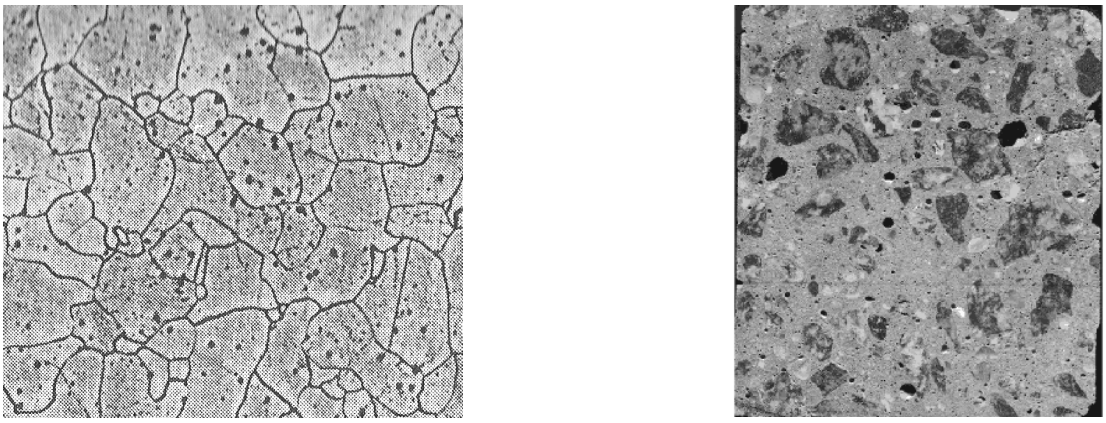

(a) (b)

Figure 1: (a) Micrograph of pure iron with ferrite inclusions and crystals having a polygonal shape. (b) Typical concrete material with aggregates, cement paste and voids.

The modelling rationale here adopted to describe the inhomogeneities contained in the material is based on a periodic distribution of spherical particles embedded in the base material. By considering, for the sake of simplicity, a single inclusion of radius embedded in an infinite plane under remote uniform stress (Fig. 2), the elastic stress field can be determined by applying the superposition principle together with the Kirsch solution [6]. The resulting stress field, $\overline{\sigma}_x$, $\overline{\sigma}_y$, $\overline{\tau}_{xy}$, is uniform within the inclusion, and can be expressed as a fraction of the remote applied stress σ_{0y}:

$$\overline{\sigma}_x = k_x \cdot \sigma_{0y}, \quad \overline{\sigma}_y = k_y \cdot \sigma_{0y}, \quad \overline{\tau}_{xy} = 0 \tag{1}$$

On the other hand, the stress field $\sigma_x, \sigma_y, \tau_{xy}$ under plane stress condition in the region around the inclusion (see point P in Fig. 2) can be expressed as follows [6]:

$$\sigma_x = \sigma_{0y}\cdot\left[\frac{(1-k_y+k_x)R^2}{2r^2}\cdot\left(3-\frac{3R^2+18y^2}{r^2}+F-G\right)+\frac{k_xR^2}{r^2}\left(1-\frac{2y^2}{r^2}\right)\right]$$
$$\sigma_y = \sigma_{0y}\cdot\left[1+\frac{(1-k_y+k_x)R^2}{2r^2}\cdot\left(1+\frac{3R^2+10y^2}{r^2}-F+G\right)-\frac{k_xR^2}{r^2}\left(1-\frac{2y^2}{r^2}\right)\right] \quad (2)$$
$$\tau_{xy} = \sigma_{0y}\cdot\left[\frac{(1-k_y+k_x)R^2xy}{r^4}\cdot\left(3-\frac{6R^2+8y^2}{r^2}+\frac{12R^2y^2}{r^4}\right)+\frac{2k_xR^2xy}{r^4}\right]$$

where $r=\sqrt{x^2+y^2}$. The x-y coordinate system has origin in the inclusion centre (Fig. 2). Further, the coefficients k_x, k_y depend on the elastic constants of the base material (E_1,ν_1) and of the inclusion (E_2,ν_2) [6]:

$$k_x = \frac{c\cdot E_2\left[(3\nu_2-1)E_1+(1-3\nu_1)E_2\right]}{E_2^{\,2}(8c^2+2c\nu_1-6c+1-\nu_1^{\,2})+E_1^{\,2}(1-\nu_2^{\,2})+E_1E_2(2\nu_1\nu_2-2+6c-2c\nu_2)} \quad (3a)$$
$$k_y = \frac{c\cdot E_2\left[E_1(3-\nu_2)+E_2(8c-3+\nu_1)\right]}{E_2^{\,2}(8c^2+2c\nu_1-6c+1-\nu_1^{\,2})+E_1^{\,2}(1-\nu_2^{\,2})+E_1E_2(2\nu_1\nu_2-2+6c-2c\nu_2)}$$

with $c=1-\nu_1^2$, and

$$F=\frac{8y^2(3R^2+2y^2)}{r^4},\quad G=\frac{24R^2y^4}{r^6} \quad (3b)$$

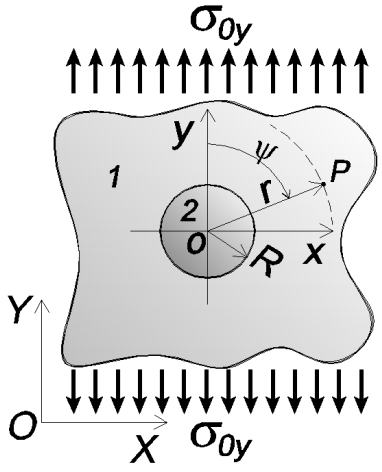

Figure 2: Circular elastic inclusion in an infinite elastic plane under remote uniform tensile stress σ_{0y}.

The elastic stress field in such heterogeneous materials can be computed by exploiting both Eqs 1-3 for a single inclusion and the superposition principle, provided that the inclusions are assumed to be non-interacting (as reasonably occurs for widely spaced inclusions).
By considering point P belonging to the base material (Fig. 3), the resulting stress field is determined approximately by summing up the effects of the inclusions (such as particles 1, 2, 3, 4, etc. in Fig. 3), that is:

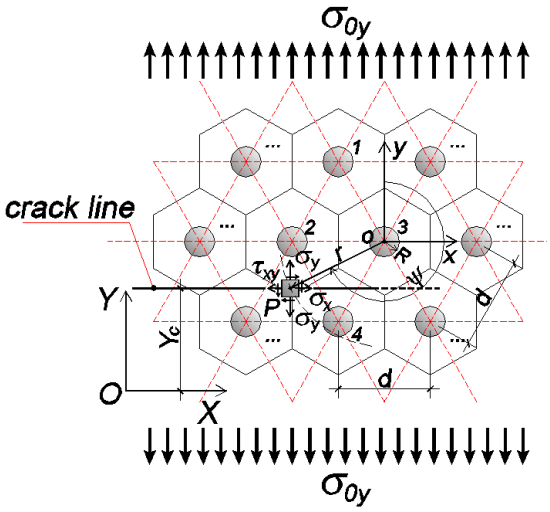

Figure 3: Equally-spaced circular inclusions in an infinite domain arranged in a hexagonal cell pattern having characteristic size d, under remote uniform tensile stress σ_{0y}.

$$\sigma_x(P) = \sum_i \sigma_{(i)x}(r_{(i)P},\theta_{(i)P})$$

$$\sigma_y(P) = \sigma_{0y} + \sum_i \left[\sigma_{(i)y}(r_{(i)P},\theta_{(i)P}) - \sigma_{0y}\right] \qquad (4)$$

$$\tau_{xy}(P) = \sum_i \tau_{(i)xy}(r_{(i)P},\theta_{(i)P})$$

where the cartesian stress tensor components $\sigma_{(i)x}(r_{(i)P},\theta_{(i)P})$, $(\sigma_{(i)y}(r_{(i)P},\theta_{(i)P})-\sigma_{0y})$, $\tau_{(i)xy}(r_{(i)P},\theta_{(i)P})$ indicate the stress fluctuations evaluated in P in an elastic infinite plane containing a single inclusion i $(i=1,2,3,4,.....)$, see Eq. 2, under the remote stress σ_{0y}. In the above expressions, the summation might be performed by taking into account all the inclusions that are within a significant influence region around the point P under consideration, since the inclusions located at a sufficiently large distance from P produce vanishing fluctuations of the stress components. In Fig. 4, sample spatial distributions of the fluctuating stress components along different lines normal to the remote loading axis are shown.

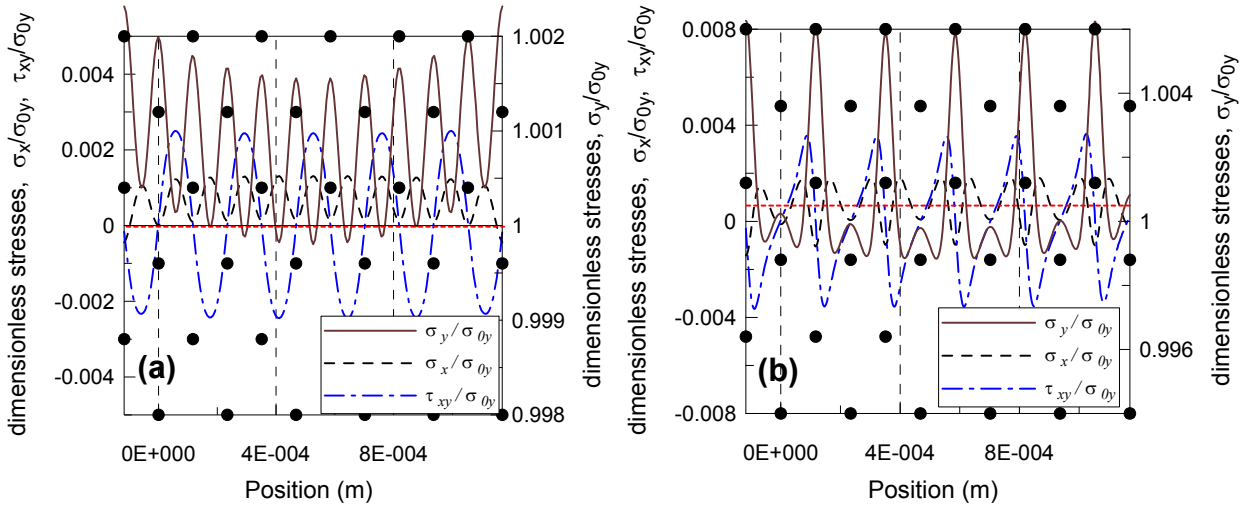

Figure 4: Stresses along a horizontal straight path (dashed line) located at (a) half distance and (b) one-third distance between two lines of inclusions, in an infinite plane under plane stress remote uniform tension stress σ_{0y}. Dots indicate the positions of inclusions in the material.

APPROXIMATE SIFS FOR A NOMINALLY-MODE I KINKED CRACK

In the case of an infinite cracked plane under a uniform remote stress σ_{0y}, the SIF of a straight crack of semi-length l aligned with the X-axis is $K_I^{(\infty)} = \sigma_{0y}\sqrt{\pi l}$.

Assume that such a straight crack is embedded in the stress field (given by Eqs 2-4) within the base material. Such a stress field can be decomposed in the remote uniform uniaxial tensile stress σ_{0y} and a fluctuating multiaxial stress field $\tilde{\mathbf{T}}(x)$ here assumed to be a one-dimensional function of the x coordinate. Furthermore, by observing the courses (reported in Fig. 4) of the stress components due to the presence of inclusions, we can suppose that $\tilde{\mathbf{T}}(x)$ is a self-balanced microstress field characterized by a material length d (related to the inclusion spacing), with two non-zero stress components $\tilde{\sigma}_y = \tilde{\sigma} = f(x/d)\tilde{\sigma}_a$ and $\tilde{\tau}_{xy} = \tilde{\tau} = f(x/d)\tilde{\tau}_a$. For the sake of simplicity, we assume $f(x/d) = \cos(2\pi x/d)$ (this could be regarded as a first order approximation through Fourier series of a general periodic function), Fig. 5a.

Under the self-balanced microstresses $\tilde{\sigma}$ and $\tilde{\tau}$, the SIFs (of the projected crack) are obtained using Buckner's superposition principle:

$$\tilde{K}_I = 2\sqrt{\frac{l}{\pi}}\int_0^l \frac{\tilde{\sigma}}{\sqrt{l^2-x^2}}dx = 2\tilde{\sigma}_a\sqrt{\frac{l}{\pi}}\int_0^l \frac{f(x/d)}{\sqrt{l^2-x^2}}dx = 2\tilde{\sigma}_a\sqrt{\frac{l}{\pi}}\int_0^l \frac{\cos(2\pi x/d)}{\sqrt{l^2-x^2}}dx = \tilde{\sigma}_a\sqrt{\pi l}\,J_0\left(\frac{2\pi l}{d}\right)$$

$$\tilde{K}_{II} = 2\sqrt{\frac{l}{\pi}}\int_0^l \frac{\tilde{\tau}}{\sqrt{l^2-x^2}}dx = 2\tilde{\tau}_a\sqrt{\frac{l}{\pi}}\int_0^l \frac{f(x/d)}{\sqrt{l^2-x^2}}dx = 2\tilde{\tau}_a\sqrt{\frac{l}{\pi}}\int_0^l \frac{\cos(2\pi x/d)}{\sqrt{l^2-x^2}}dx = \tilde{\tau}_a\sqrt{\pi l}\,J_0\left(\frac{2\pi l}{d}\right) \quad (5)$$

where J_0 is the zero-order Bessel function [7].

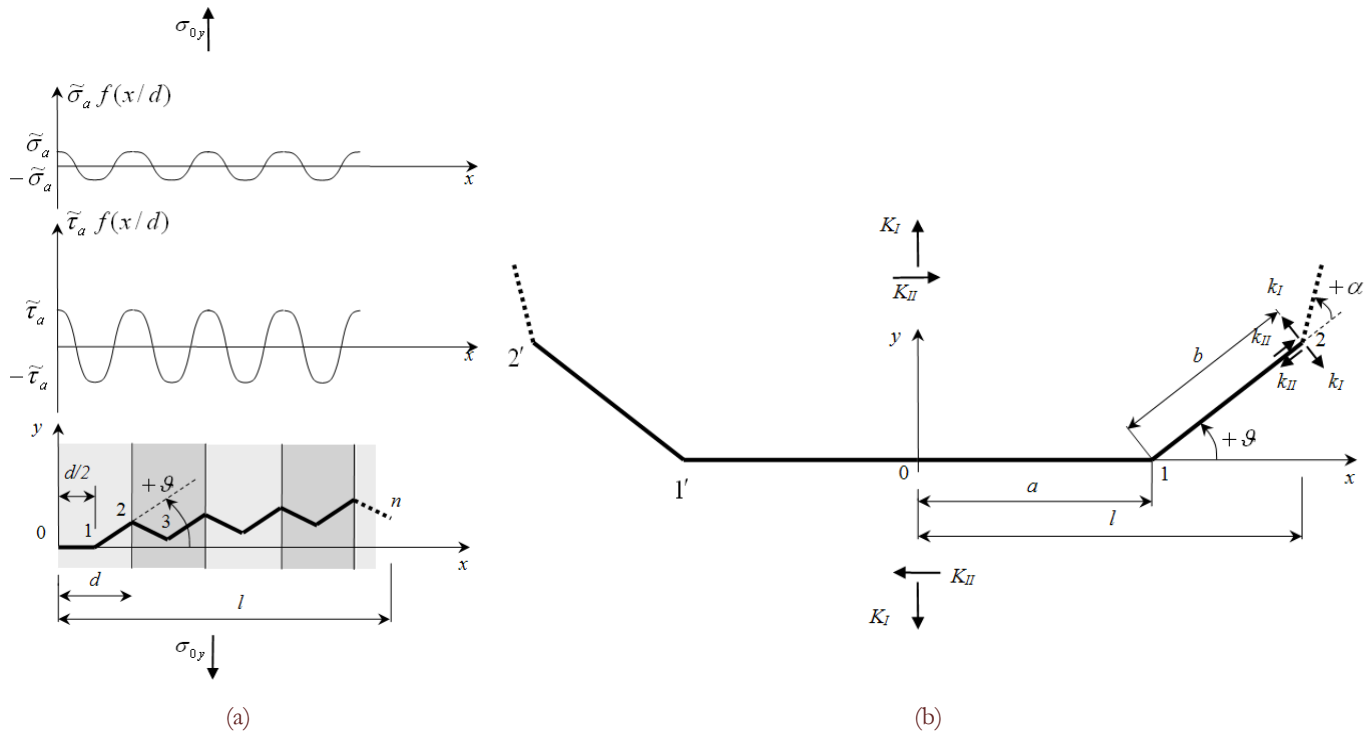

(a) (b)

Figure 5: (a) Self-balanced microstress field and periodically kinked crack. (b) Kinked crack in an infinite plane.

The total SIFs of the straight crack with semi-length l are the sums of the two contributions due to remote and microstress fields, that is:

$$K_I = K_I^{(\infty)} + \tilde{K}_I$$
$$K_{II} = K_{II}^{(\infty)} + \tilde{K}_{II} \tag{6}$$

In the self-balanced microstress field, we assume that the crack might kink at each material microstructure semi-period, namely at each reversal in the microstress spatial courses. Obviously, kinking occurs since the microstress field is multiaxial. Because of the symmetry condition related to the Y-axis, the crack propagates symmetrically with respect of such an axis. Now, considering at first a singly-kinked crack (of projected crack length $2l$), we have that the SIFs at the tips of the inclined part of the crack can be expressed through the SIFs K_I and K_{II} of a straight crack of length equal to the projected length of the kinked crack [8,9], that is:

$$k_I = a_{11}\left(\vartheta, b/a\right)K_I + a_{12}\left(\vartheta, b/a\right)K_{II}$$
$$k_{II} = a_{21}\left(\vartheta, b/a\right)K_I + a_{22}\left(\vartheta, b/a\right)K_{II} \tag{7}$$

where a_{ij} are coefficients which depend on the slant angle ϑ (positive counter-clockwise for tip coordinate x > 0) and the length ratio b/a between the deflected leading segment and the horizontal trailing (preceding) segment (Fig. 5). If a geometry different from that of an infinite plate with a central crack were examined, the SIFs defined with respect to the projected crack would change but not the expressions in Eq. 7.
The coefficients a_{ij} for $b/a \to \infty$ (and, with good approximation, also for $b/a > 0.3$) are [8]:

$$a_{11}\left(\vartheta\right) = \cos^{3/2}\vartheta$$
$$a_{12}\left(\vartheta\right) = -2\sin\vartheta\cos^{1/2}\vartheta$$
$$a_{21}\left(\vartheta\right) = \sin\vartheta\cos^{1/2}\vartheta$$
$$a_{22}\left(\vartheta\right) = \cos 2\vartheta\cos^{-1/2}\vartheta \tag{8}$$

Note that the local SIFs in Eq. 8 are equal to those of an inclined straight crack of projected semi-length l forming an angle $\pi/2 - \vartheta$ with respect to the loading axis of $\sigma_{0,y}$ [8], Fig. 6.

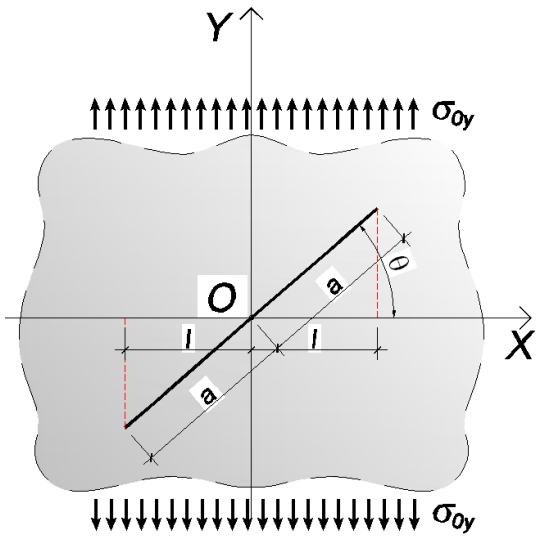

Figure 6: Infinite cracked plane with an inclined crack under remote tensile stress $\sigma_{0,y}$.

Then, we assume that, as the crack propagates following the path in Fig. 5a, only the latter deflection of the crack path influences the stress field near the crack tips (e.g. along the straight segment 2-3 in Fig. 5a, the deflection point 2 has an

effect, while the deflection point 1 does not have). The local SIFs at the crack tip are assumed to be given by Eqs 7 and 8 for deflected (Mode I+II) segments (the segments 1-2 and $1'-2'$ in Fig. 5b).
The approximate calculation (based on the assumption that the near-tip stress field depends on the local crack direction at the crack tip) of the local SIFs for the kinked crack is examined for the case of an edge cracked plane under uniform tensile stress, Fig. 7a [10]. In particular, a two-equal-segment kinked crack with $\theta_1 = 45°$ and θ_2 ranging from 0° to 60° is considered. In Fig. 7b, we can observe that the SIFs computed by means of a FE model agree quite satisfactory with the analytical values corresponding to an equivalent slant straight crack (see thin line in Fig. 7a) having both the direction of the leading segment of the kinked crack and a projected length (normal to the loading axis) equal that of the kinked crack.

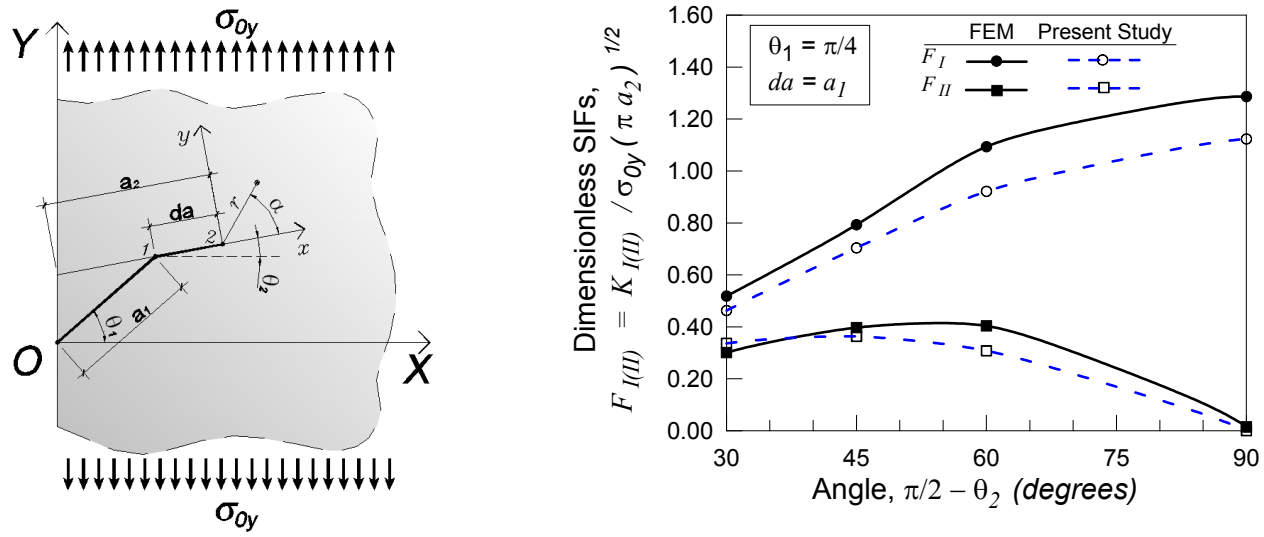

(a) (b)

Figure 7: (a) Edge-cracked plane. (b) SIFs obtained from the simplified method (present study, dashed line) and a FE analysis (continuous line) for a two-segment crack.

MIXED-MODE CRACK PROPAGATION CRITERIA

The kinked pattern of a crack embedded in the microstress field above described (see Sections 2 and 3) can be analysed by adopting a mixed-mode crack propagation criterion. Several criteria for both stable and unstable crack propagation have been proposed during the last decades for different materials.
According to the *MTS-criterion* (Maximum Tensile Stress) proposed by Erdogan and Sih [2, 3], the crack grows in the direction perpendicular to the maximum principal stress (σ_α) direction or, equivalently, parallel to the maximum tangential stress. Analytically, the criterion can be stated as follows:

$$\frac{\partial \sigma_\alpha}{\partial \alpha} = 0, \quad \frac{\partial^2 \sigma_\alpha}{\partial \alpha^2} < 0 \tag{9}$$

where the polar coordinate α is used to identify the position vector with respect to the crack tip direction. By means of the stress field expressions (2), Eq. 9 can be written as follows:

$$\tan^2 \frac{\alpha}{2} - \frac{\mu}{2} \tan \frac{\alpha}{2} - \frac{1}{2} = 0 \quad \text{with} \quad \mu = k_I / k_{II} \tag{10}$$

This classical criterion, used to describe the mixed-mode crack propagation under the local SIFs k_I and k_{II}, provides a kinking angle α, defined with respect to the general inclined axis of the crack, given by:

$$\alpha = 2 \arctan \left[\frac{1}{4} \frac{k_I}{k_{II}} \pm \frac{1}{4} \sqrt{\left(\frac{k_I}{k_{II}} \right)^2 + 8} \right] \tag{11}$$

Several others criteria have been proposed, for instance the *zero shear stress criterion* by Maiti et al. [11], the *M-criterion* proposed by Kong et al. [12] based on the maximum value of the stress triaxiality ratio $M = \sigma_H / \sigma_{eq}$ (σ_H is the hydrostatic stress, whereas σ_{eq} is an equivalent stress which can be assumed to be equal to the Von Mises stress), the maximum dilatational strain energy density criterion (*T-criterion*) proposed by Theocaris et al. [13-15].
From experimental tests, it has been observed that the crack propagation direction usually tends to follow the local or global minimum extension of the plastic core region. From a physical point of view, this phenomenon could be explained by considering that the plastic core region is a highly-strained area, and the crack tends to reach the elastic region of the material outside the plastic zone, propagating through the plastic region which develops around the crack tip. Therefore, it is reasonable to assume that the crack follows the "easiest" path to reach the elastic region. Such a path can be assumed to coincide with the shortest path from the crack tip to the elastic material outside the plastic zone, as is stated by the *R-criterion* proposed by Shafique et al. [4, 5] (Fig. 8). The *R-criterion* can mathematically be written as follows :

$$\frac{\partial R_p}{\partial \alpha} = 0, \qquad \frac{\partial^2 R_p}{\partial \alpha^2} > 0 \tag{12}$$

where R_p is the function which defines the radial distance from the crack tip to a generic point of the plastic zone boundary $F(I_1, J_2) = 0$, with I_1 = first stress tensor invariant and J_2 = second deviatoric stress tensor invariant. When the conditions stated in Eq. 12 are fulfilled, the direction of minimum radial distance is determined, and the crack propagation direction vector $\mathbf{t}$ is assumed to be coincident with such a direction (Fig. 8).

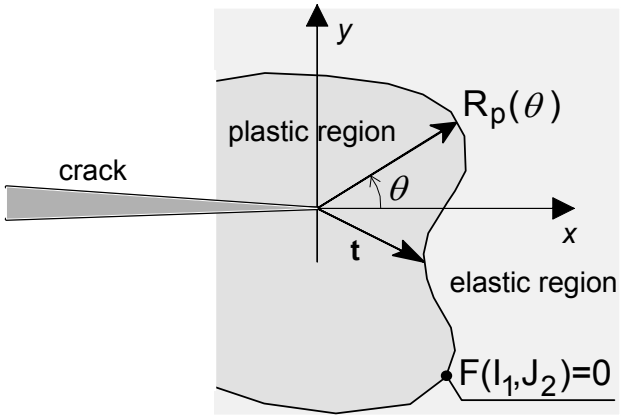

Figure 8: Graphical representation of the R-criterion.

The above criterion can also be justified by considering that the fracture stress σ_f is proportional to the square root of w_f, which is the fracture energy per unit surface area. Such an energy for a quasi-brittle elastic-plastic material is equal to the summation of the surface energy γ_s and the plastic work γ_p consumed to create a unit surface area, that is, $w_f = \gamma_s + \gamma_p$. For structural materials, where typically $\gamma_p >> \gamma_s$, the fracture stress σ_f appears to be primarily dependent on γ_p only. The shortest distance from the crack tip to the elastic-plastic boundary corresponds to the minimum plastic work which is needed to create a new portion of crack area, that is, such a shortest distance corresponds to the minimum values of fracture energy and fracture stress.

APPLICATIONS TO SHORT-CRACK PROPAGATION REGIME

The above described model for the assessment of crack propagation at the microscale is herein applied to a carbon steel D6ac whose composition and mechanical parameters are presented in Tab. 1, where only the main secondary elements are listed.
By performing a weighted average of the physical and mechanical parameters of the secondary constituents, a single equivalent inclusion with the features reported in Tab. 2 can be defined.

	Element	volume fraction η [%]	Mass density ρ [kg/m³]	Young modulus E [Gpa]	Poisson's ratio ν	Thermal expansion coeff. α [K⁻¹]
Iron	Fe	~ 98.00	7870	200	0.29	1.20E-05
Molibden	Mb	~ 1.05	10220	330	0.38	5.35E-06
Cromium	Cr	~ 1.05	7190	248	0.30	6.20E-06

Table 1: Physical and mechanical parameters of the main elements in a carbon steel D6ac.

	Element	volume fraction η [%]	Mass density ρ [kg/m³]	Young modulus E [GPa]	Poisson's ratio ν	Thermal expansion coeff. α [K⁻¹]
Base material	Fe	~ 98.00	7870	200	0.29	1.20E-05
Equivalent inclusion	--	~ 2.10	8705	289	0.34	5.78E-06

Table 2: Mean physical and mechanical parameters of the base material and the equivalent inclusion in a carbon steel D6ac.

Now consider an infinite plane under remote uniform tensile stress σ_{0y}, containing an initial straight crack normal to the applied stress. By adopting the equivalent inclusion volume fraction (Tab. 2) and considering an average inclusion diameter equal to about $20\mu m$ (e.g. see Ref. [16]), an inclusion spacing d equal to about $234\mu m$ can be computed for a regular hexagonal distribution of inclusions (Fig. 3). The static crack extension is determined by applying the above described criteria (the Erdogan-Sih criterion and the R-criterion) on the crack growth direction.
The mixed mode SIFs are computed by taking into account only the remote stress σ_{0y} (the local fluctuation of the stress component σ_y is negligible, as is shown in Fig. 4) and the micro shear stress fluctuations $\tilde{\tau}$. In Fig. 9, the crack path predicted for an initially straight crack developing at half distance between two horizontal lines of inclusions (see Fig. 4a, with $|\tilde{\tau}_a|/\sigma_{y0} \cong 0.0026$) is represented. The crack path evaluated by the Erdogan-Sih criterion is similar to that determined by the R-criterion (Fig. 9). Nevertheless, it can be observed that the R-criterion produces a slight crack path deviation since the plastic zone shape is influenced in a complex way by the Mode I and Mode II SIFs which continuously change during the whole process of crack propagation.

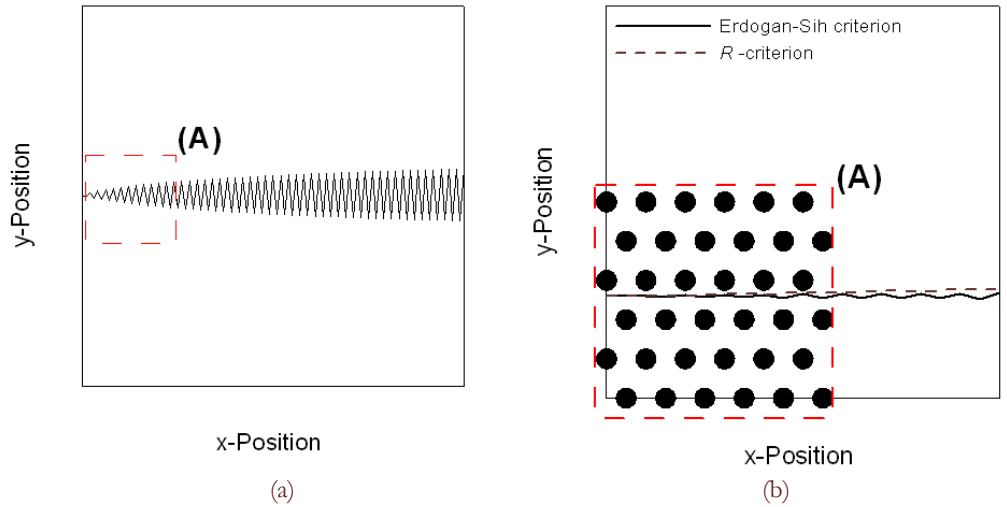

Figure 9: (a) Path of an initially straight crack developing at half distance between two lines of inclusions in an infinite plane under remote uniform tensile stress σ_{0y}. (b) Detail of the crack path at the microscale where the distribution of inclusions is shown.

Fig. 10 shows the crack path determined for an initially straight crack developing at a vertical distance equal to one-third between two horizontal lines of inclusions (see Fig. 4b, with $|\tilde{\tau}_a|/\sigma_{y0} \cong 0.0037$). As in the previous case, the crack path evaluated by the Erdogan-Sih criterion is rather similar to that determined by the R-criterion.

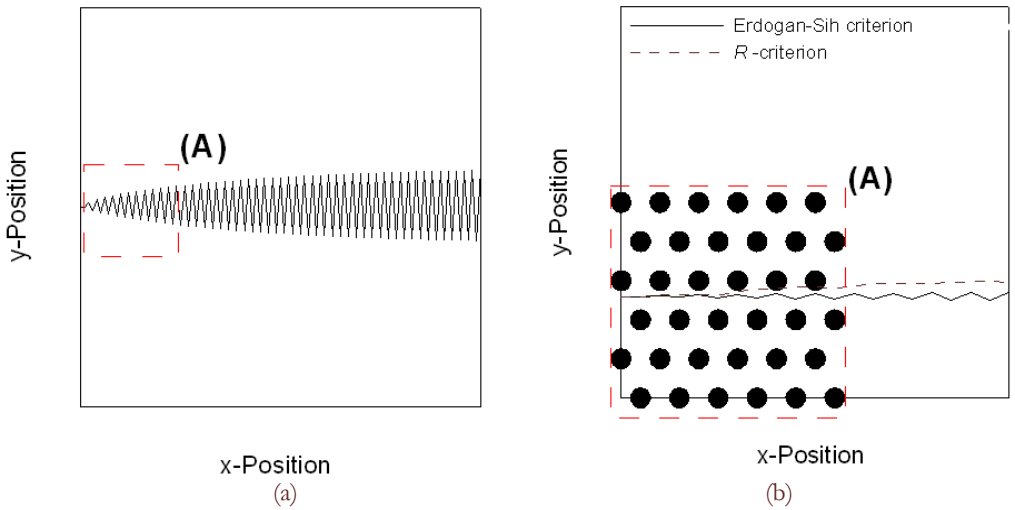

Figure 10: (a) Path of an initially straight crack developing at one-third distance between two lines of inclusions in an infinite plane under remote uniform tensile stress σ_{0y}. (b) Detail of the crack path at the microscale where the distribution of inclusions is shown.

By comparing Fig. 9 and Fig. 10, it can be observed that the kinking angle of the crack tends to increase with increasing the value of the $|\tilde{\tau}_a|/\sigma_{0y}$ ratio.

CONCLUSIONS

In the present paper, a simple analytical model to describe the trajectory of a plane crack propagating within an inhomogeneous material is proposed. With reference to metals, the inhomogeneities are treated by considering a two-phase material with an equivalent mean inclusion characterized by a regular spatial distribution. Even under remote uniaxial loading, the equivalent inclusions generate a multiaxial fluctuating stress field which is assumed to be responsible for mixed-mode crack propagation.

By adopting different mixed-mode crack growth criteria, the crack path can be connected with the main features of the material microstructure, here accounted in terms of an appropriate microstress field. It is shown that both the maximum principal stress criterion and the *R*-criterion (based on the minimum extension of the core plastic zone) predict a zig-zag crack pattern, characterised by a length scale related to both the volume fraction of inclusions and their mean size. Moreover, it is shown a strong dependence of the crack path on the material microstructure in the short crack regime, while the microstructure of the material does not influence the crack trajectory for relatively long cracks.

ACKNOWLEDGEMENTS

The authors gratefully acknowledge the research support for this work provided by the Italian Ministry for University and Technological and Scientific Research (MIUR).

REFERENCES

[1] S. Suresh Metallurgical Trans, 14A (1985) 2375.
[2] F. Erdogan, G. C. Sih, J Basic Engng, 85 (1963) 519.

[3] G.C. Sih, Int. J. Fract, 10 (1974) 305.
[4] M.A.K. Shafique, K. K. Marwan, Engng Fract Mech, 67 (2000) 397.
[5] M.A.K. Shafique, K. K. Marwan, Int. J Plasticity, 20 (2004) 55.
[6] Ye.Ye. Deryugin, G.V. Lasko, S. Schmauder, Field of stresses in an isotropic plane with circular inclusion uncere tensile stress (http://www.ndt.net/article/cdcm2006/papers/lasko.pdf)
[7] A.Carpinteri, A. Spagnoli, S. Vantadori, In: The 13th Int. Congress on Mesomechanics (Mesomechanics 2011), 6-8 July 2011, Vicenza (Italy).
[8] H. Kitagawa, R. Yuuki, T. Ohira, Engng Fract Mechs, 7 (1975) 515.
[9] YZ. Chen, Theoretical Applied Fract Mech, 31 (1999) 223.
[10] A. Carpinteri, R. Brighenti, S. Vantadori, D. Viappiani, Special Issue Engng Fract Mech, 75 (3-4) (2007) 510.
[11] S. K.Maiti, R. A. Smith, Int J Fract, 23 (1983) 281.
[12] X. M. Kong, M. Schulter, W. Dahl, Engng Fract. Mech. , 52 (1995) 379.
[13] P. S. Theocaris, NP. Adrianopoulos, Engng Fract Mech, 16 (1982) 425.
[14] P. S.Theocaris, G. A. Kardomateas, NP. Adrianopoulos, Engng Fract. Mech, 17 (1982) 439.
[15] P. S. Theocaris, NP. Adrianopoulos, Int. J. Fract, 20 (1982) R125.
[16] Y. Murakami, Metal Fatigue: Effects of Small Defects and Nonmetallilc Inclusions. Elsevier, Amsterdam, (2002).